A corrected version of THE FARMER COSMOS2020 catalogue

J. R. Weaver, O. B. Kauffmann, O. Ilbert, H. J. McCracken, A. Moneti, S. Toft, G. Brammer, M. Shuntov, I. Davidzon, B. C. Hsieh, C. Laigle, A. Anastasiou, C. K. Jespersen, J. Vinther, P. Capak, C. M. Casey, C. J. R. McPartland, B. Milvang-Jensen, B. Mobasher, D. B. Sanders, L. Zalesky, S. Arnouts, H. Aussel, J. S. Dunlop, A. Faisst, M. Franx, L. J. Furtak, J. P. U. Fynbo, K. M. L. Gould, T. R. Greve, S. Gwyn, J. S. Kartaltepe, D. Kashino, A. M. Koekemoer, V. Kokorev, O. Le Fèvre, S. Lilly, D. Masters, G. Magdis, V. Mehta, Y. Peng, D. A. Riechers, M. Salvato, M. Sawicki, C. Scarlata, N. Scoville, R. Shirley, J. Silverman, A. Sneppen, V. Smolčić, C. Steinhardt, D. Stern, M. Tanaka, Y. Taniguchi, H. I. Teplitz, M. Vaccari, W.-H. Wang, G. Zamorani

March 5, 2023

1 Abstract

COSMOS2020 (Weaver et al. 2022) consists of two catalogues named THE FARMER and CLASSIC, both containing photometry in around 40 bands and quantities such as photometric redshifts derived from SED fits. The two catalogues were released in June 2022 via ESO's Phase 3 system in the UltraVISTA collection under the label DR4.1. We have recently discovered a minor bug in THE FARMER catalogue: the magnitude errors in the catalogue are moderately too small in the large error regime: for example, a reported error of 0.7 mag should have been 1.0 mag. The flux errors and all derived quantities such as photo-zs are not affected, and the CLASSIC catalogue is not affected. The present release, with label DR4.1.1, contains a corrected version of THE FARMER catalogue.

1.1 Acknowledging these data products

If you use these catalogues, please cite the following paper: "COSMOS2020: A panchromatic view of the Universe to $z \sim 10$ from two complementary catalogues", Weaver et al. (2022). You must also include the following standard acknowledgement:

"Based on observations collected at the European Southern Observatory under ESO programme ID 179.A-2005 and on data products produced by CALET and the Cambridge Astronomy Survey Unit on behalf of the UltraVISTA consortium."

If the access to the ESO Science Archive Facility services was helpful for you research, please include the following acknowledgement: "This research has made use of the services of the ESO Science Archive Facility."

You are additionally encouraged to cite the papers describing the data sets included in the catalogue (such as McCracken et al. 2012 for UltraVISTA).

2 Changes with respect to previous versions

2.1 Changes from COSMOS2015 to COSMOS2020

The previous COSMOS catalogue was COSMOS2015 (Laigle et al. 2016). It was released in Phase 3 under the label UltraVISTA DR2.1, as the catalogue was based on the UltraVISTA DR2 imaging. It was the first COSMOS catalogue to be released via Phase 3. COSMOS2015 consisted of a single catalogue. COSMOS2020 (Weaver et al. 2022) consists of two catalogues, called CLASSIC and THE FARMER (see Sect. 3.2). COSMOS2020 is based on the UltraVISTA DR4 imaging, and was first released in Phase 3 under the label UltraVISTA DR4.1 (see Sect. 2.2). The present release (DR4.1.1) fixes a minor bug in THE FARMER catalogue (see Sect. 2.3).

2.2 Changes from the initial public non-Phase 3 version of COSMOS2020 to the first Phase 3 version (DR4.1)

The COSMOS2020 catalogues and supporting files were initially made publicly available on our website `https://cosmos2020.calet.org/` when the Weaver et al. paper appeared on arXiv on 28 Oct 2021 (`https://arxiv.org/abs/2110.13923`). We subsequently made an updated version, as described in Sect. 2.2.1 and 2.2.2 below. This version was released via Phase 3, and has since 24 Jun 2022 also been made available on our website, replacing the initial version.

2.2.1 Bug fixes and minor improvements

Many of the following changes were not directly due to Phase 3 requirements, but were often a result of our work preparing the Phase 3 release, and some of the bugs were discovered by ESO's Phase 3 scientist Laura Mascetti.

- CLASSIC: negative values in the column `FLUX_RADIUS` were set to NaN

- THE FARMER: corrected the column names for the four `ACS_F814W` columns (which lacked the `ACS_` part)

- THE FARMER: added columns `MODEL_FLAG` and `GROUP_ID`, and removed column `VALID_SOURCE` (which was not needed after the introduction of column `MODEL_FLAG`)

- THE FARMER: set all column values to NULL for sources that moved more than $0.6''$ from their detection position (these sources can be identified by the `MODEL_FLAG` column being set to 2)

- THE FARMER: column `SOLUTION_MODEL` was empty, now fixed

- CLASSIC and THE FARMER: added the `ez_ssfr` column

- CLASSIC and THE FARMER: the value of the `TNULL` keywords were changed from two incorrect values to the intended value of -99

- CLASSIC and THE FARMER: the column `lp_age` was missing a unit (`TUNIT`), now fixed

- CLASSIC and THE FARMER: The catalogues contain the columns `ez_mass` (log stellar mass), `ez_sfr` (log SFR), and `ez_Lv` (log V-band luminosity). For each of these physical quantities the catalogues also contain five percentile columns, e.g. `ez_mass_p025` for the 2.5% percentile. Before the change, the values in these 3×5 percentile columns corresponded to the linear version of the quantity, while after the change they correspond to the logarithmic version

- CLASSIC and THE FARMER: the columns `lp_age`, `lp_dust`, `lp_mass_best`, `lp_SFR_best` and `lp_sSFR_best` used -99.9 to indicate NULL, which was changed to NaN

- CLASSIC: the columns `SPLASH_CH1_MAG`, `SPLASH_CH2_MAG`, `SPLASH_CH3_MAG`, `SPLASH_CH4_MAG`, `SPLASH_CH1_MAGERR`, `SPLASH_CH2_MAGERR`, `SPLASH_CH3_MAGERR` and `SPLASH_CH4_MAGERR` used -99.9 to indicate NULL, which was changed to NaN

2.2.2   Changes directly related to the Phase 3 requirements

All of the following changes relate only to the header part of the FITS files, not to the data part. These changes were made so that the data products meet the requirements defined in the ESO Science Data Products Standard document, available from the Phase 3 website[1].

- The required metadata were added to the primary headers. This includes metadata relevant to the ESO data only (here the UltraVISTA DR4 imaging in the 5 bands), such as provenance, time span, ESO programme IDs, filter names and limiting magnitudes, and metadata relevant to the catalogue as a whole, such as the footprint on the sky and the bibcode for the paper to be referenced

- For each of the almost 1200 columns in the two catalogues we wrote a description of length up to 68 characters; these descriptions are probably quite useful to the typical user. The descriptions are found in the extension 1 FITS headers (in the `TCOMM` keywords) and are listed in this document in Appendix 6.1 and 6.2

- For each column we also wrote a Unified Content Descriptor Version 1+ (UCD1+)[2]. This is a standardised vocabulary. An example could be `stat.error;phot.mag;em.opt.R` which means a statistical error on a photometric magnitude for electromagnetic radiation between 600 and 750 nm. Writing the UCDs was a substantial and complex task, and we acknowledge discussions with ESO and the IVOA Semantics group. These UCDs are found in the extension 1 header (in the `TUCD` keywords), but not given here in this document

- The extension 1 headers already contained units (in the `TUNIT` keywords), but expressed in the format/syntax of the `astropy` package (Robitaille et al. 2013; Astropy Collaboration et al. 2018). The units were changed to follow the ESO standard (see Sect. 8 of the ESO Data Interface Control Document[3]), which implements a subset of the IVOA standard[4]. The updated units are in the `TUNIT` keywords and are also listed in Appendix 6.1 and 6.2.

---

[1] https://www.eso.org/sci/observing/phase3.html
[2] https://www.ivoa.net/documents/UCD1+/
[3] https://archive.eso.org/cms/tools-documentation/eso-data-interface-control.html
[4] https://ivoa.net/documents/VOUnits/

Examples of changes:
```
pix2 → pix**2
dex(solLum) → log(solLum)
solLum-1 solMass → solMass/solLum
```

We verified the correctness of the UCDs and units using STILTS (Taylor 2006), using votlint[5] and the VO-tools[6] (based on ucidy[7] and unity[8]), and the overall Phase 3 verification was performed by ESO. The files with the updates described in this and the previous subsections were named `R1_v2.1_p3` and are released via this ESO Phase 3 release. (See the note on filenames in Sect. 4.)

2.3   Changes from DR4.1 to DR4.1.1

We recently (early 2023) discovered that the magnitude errors in the COSMOS2020 THE FARMER catalogue released in DR4.1 (filename `COSMOS2020_FARMER_R1_v2.1_p3.fits`) are moderately too small in the large error regime: for example, a reported error of 0.7 mag should have been 1.0 mag, as shown in Fig. 1. The bug was due to an editing error in the Python code.
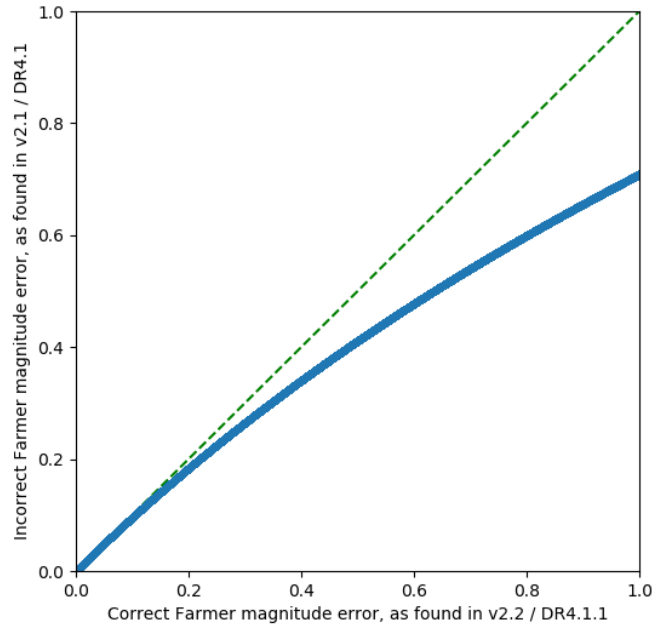
Figure 1: Comparison of magnitude errors in the two versions of THE FARMER COSMOS2020 catalogue.
x-axis: Correct THE FARMER magnitude error, as found in v2.2 / DR4.1.1, and
y-axis: Incorrect THE FARMER magnitude error, as found in v2.1 / DR4.1.
The green dashed line marks the one-to-one relation.

---

[5] http://www.star.bristol.ac.uk/~mbt/stilts/sun256/votlint.html

[6] http://www.star.bristol.ac.uk/~mbt/stilts/sun256/uk.ac.starlink.ttools.func.VO.html

[7] https://github.com/gmantele/ucidy

[8] https://code.nxg.name/nxg/unity

The flux errors and all derived quantities such as photo-zs are not affected, and the Classic catalogue is not affected. The present release, with label DR4.1.1 and with files named v2.2, contains a corrected version of The Farmer catalogue (filename `COSMOS2020_FARMER_R1_v2.2_p3.fits`).

The present release does does include the Classic catalogue: please obtain that from the DR4.1 release via the usual ESO interfaces. The release description document for DR4.1 can be found at `https://eso.org/rm/api/v1/public/releaseDescriptions/195` .

3   Release notes

In the following Sections, a highly condensed description of both catalogues is presented. For full details, see Weaver et al. (2022).

3.1   COSMOS2020 imaging data

The principal improvements in COSMOS2020 compared to previous COSMOS catalogues and the previous ESO Phase 3 COSMOS catalogue are the significantly deeper optical and near-infrared images from ongoing Subaru-HSC and VISTA-VIRCAM surveys. In addition, this release contains the definitive reprocessing of all Spitzer data ever taken on COSMOS. 'Legacy' or pre-existing data sets present in the previous COSMOS2015 catalogue have been reprocessed to take advantage of improved astrometry from Gaia (the only exceptions being external ancillary data such as GALEX). All images are resampled to final stacks with a $0''15$ pixel scale. These stacks are aligned to the COSMOS tangent point, which has a right ascension and declination (J2000) of (10h00m27.92s $+02°12'03''50$). For full details, see Weaver et al. (2022).

3.2   Photometric measurements

For the new COSMOS2020 catalogues, two independent photometric catalogues are computed using two different techniques. In both cases, the input source list is made by detecting objects on a deep $izJYHK_s$ combined `CHI-MEAN` image (defined in Appendix B of Drlica-Wagner et al. 2018) generated using `SWarp`. This image is optimised for the detection of high-redshift objects.

One catalogue is generated using the same photometric measurement methods as our previous COSMOS2015 catalogue (Laigle et al. 2016). Objects are detected with `SExtractor` (Bertin & Arnouts 1996) and for each galaxy, colours are computed using using aperture photometry performed on PSF-homogenized images (except for Spitzer/IRAC bands, where PSF-fitting with the `IRACLEAN` software (Hsieh et al. 2012) is used). This is called the "Classic" catalogue.

The second photometric catalogue is created using the `The Tractor` (Lang et al. 2016) package starting from a slightly different source list derived independently with `SEP` Barbary (2016) (a `python` implementation of `SExtractor`). `The Tractor` derives parametric models from one or more images containing morphological information. An associated package, The Farmer (Weaver et al., in prep.), generates a full multi-wavelength catalogue using `The Tractor` to perform the modelling. This approach has the advantage that `The Tractor` does not require a high-resolution image and can hence be consistently applied to ground-based data sets (and

no PSF homogenization is required). Because the models are purely parametric, `The Tractor` can provide basic shape measurements for resolved sources in addition to fluxes. Detailed comparisons of both photometric catalogues and the quality of the derived photo-z are presented in Weaver et al. (2022).

Both catalogues have their advantages and disadvantages, and the choice of which catalogue to use should be made based on the scientific application in question. Having multiple photometric redshifts for a large subset of sources can also be invaluable for validation and testing of specific measurements in COSMOS.

3.3   Photometric redshifts and physical parameters

Photometric redshifts and physical parameters are computed for both catalogues using `LePhare` (Arnouts et al. 2002; Ilbert et al. 2006) and `EAZY` (Brammer et al. 2008). Results from both packages are broadly in agreement, but once again, the choice of which package to use must be made based on the scientific application in question.

3.4   Astrometric calibration

Astrometric solutions were computed for all optical, infrared and near-infrared data using the Gaia references catalogues (DR1 or DR2; Gaia Collaboration et al. (2016, 2018)). In general, the agreement between positions of sources in each of the stacks with the external references catalogues and between sources in different bands is around 10 mas and 1 mas respectively.

4   Release Content

Table 1 lists the data products (files) in this release (DR4.1.1). Table 2 gives the correspondence between the files in DR4.1.1 and in DR4.1, for reference. Note that throughout this document, the file names are the ones we have used in our upload to the ESO Phase 3 system. Upon publication in the Phase 3 system / ESO Science Archive Facility, the files are renamed `ADP` followed by a publication timestamp. As an example, the COSMOS2015 catalogue is called `ADP.2016-12-15T11:49:34.984.fits`. ADP means Advanced Data Products. The original file name is recorded in the keyword `ORIGFILE` in the primary header. One of our data products is a tar file, containing a mix of relevant files: mask files in the form of ds9 region files, and two Python code fragments. The files in the tar file are listed in Table 3. A full description of the masks is provided in Section 4.6.

Table 1: Data products delivered with this release, i.e. DR4.1.1

Filename	Description
`COSMOS2020_FARMER_R1_v2.2_p3.fits`	THE FARMER catalogue, see Section 4.4.
`COSMOS2020_FARMER_R1_v2.2_LEPHARE_PZ_p3.fits`	Redshift probability distributions, see Section 4.7
`COSMOS2020_FARMER_R1_v2.2_EAZY_CZ_p3.fits`	Redshift probability distributions, see Section 4.7
`COSMOS2020_izYJHKs_chimean-v3_COPY_p3.fits`	`CHI-MEAN` detection image
`COSMOS2020_extra_COPY_p3.tar`	Supplementary files, see Table 3

Table 2: Files in this release (DR4.1.1), and in DR4.1 for reference

File in DR4.1.1	File in DR4.1
`COSMOS2020_FARMER_R1_v2.2_p3.fits`	`COSMOS2020_FARMER_R1_v2.1_p3.fits`
`COSMOS2020_FARMER_R1_v2.2_LEPHARE_PZ_p3.fits`	`COSMOS2020_FARMER_R1_v2.1_LEPHARE_PZ_p3.fits`
`COSMOS2020_FARMER_R1_v2.2_EAZY_CZ_p3.fits`	`COSMOS2020_FARMER_R1_v2.1_EAZY_CZ_p3.fits`
`COSMOS2020_izYJHKs_chimean-v3_COPY_p3.fits`	`COSMOS2020_izYJHKs_chimean-v3_p3.fits`
`COSMOS2020_extra_COPY_p3.tar`	`COSMOS2020_extra_p3.tar`
...	`COSMOS2020_CLASSIC_R1_v2.1_p3.fits`
...	`COSMOS2020_CLASSIC_R1_v2.1_LEPHARE_PZ_p3.fits`
...	`COSMOS2020_CLASSIC_R1_v2.1_EAZY_CZ_p3.fits`

Table 3: Contents of the tar file

Filename	Description
`MASK_SUPCAM_COSMOS2020.reg`	Suprime-cam mask file.
`MASK_HSC-stars_griz_COSMOS2020.reg`	HSC mask file.
`MASK_UDEEP_COSMOS2020.reg`	Mask file for the Ultra-Deep regions.
`MASK_UVISTA_COSMOS2020.reg`	Mask file for the UltraVISTA area.
`MASKS_README.txt`	Description of the masks.
`flags_in_catalog.png`	Mask illustration (Figure 2).
`eazy_zcdf_pdf.txt`	Code fragment to compute photo-z PDFs from `EAZY` output.
`COSMOS2020_prepare_apertures.txt`	Code fragment to compute photometry from Classic catalogue.

4.1 Labels used for the various photometric datasets

The two COSMOS2020 catalogues contain photometry based on a number of datasets. For each of the 44 datasets we have assigned a label given in Table 4; this label is used in the column names (see the complete lists of columns names in Sections 6.1 and 6.2). Note that for most datasets we performed the photometry ourselves (Weaver et al. 2022), while for GALEX, ACS and SPLASH the photometry was crossmatched from external catalogues (see our README files in Sections 4.3 and 4.5).

4.2 The Classic catalogue

Not applicable because DR4.1.1 does not include the Classic catalogue (see DR4.1 for that).

4.3 Description of Classic catalogue columns

Not applicable because DR4.1.1 does not include the Classic catalogue (see DR4.1 for that).

4.4 The Farmer catalogue

THE FARMER catalogue contains 430 columns and 964,506 rows. We provide matches with ACS, X-Ray, UV, IR, FIR and radio catalogues and also with previous COSMOS catalogues and in particular COSMOS2015. Sect. 4.5 provides the README file distributed with the catalogue

Table 4: The photometric datasets

Label	Description	$\lambda_{\mathrm{central}}$ [Å]	width[Å]
GALEX_FUV	GALEX FUV	1526	224
GALEX_NUV	GALEX NUV	2307	791
CFHT_u	CFHT/MegaCam u	3709	518
CFHT_ustar	CFHT/MegaCam u*	3858	598
ACS_F814W	HST/ACS F814W	8333	2511
HSC_g	Subaru/HSC HSC-SSP PDR2 g	4847	1383
HSC_r	Subaru/HSC HSC-SSP PDR2 r	6219	1547
HSC_i	Subaru/HSC HSC-SSP PDR2 i	7699	1471
HSC_z	Subaru/HSC HSC-SSP PDR2 z	8894	766
HSC_y	Subaru/HSC HSC-SSP PDR2 y	9761	786
SC_B	Subaru/SuprimeCam B	4488	892
SC_gp	Subaru/SuprimeCam g+	4804	1265
SC_V	Subaru/SuprimeCam V	5487	954
SC_rp	Subaru/SuprimeCam r+	6305	1376
SC_ip	Subaru/SuprimeCam i+	7693	1497
SC_zp	Subaru/SuprimeCam z+	8978	847
SC_zpp	Subaru/SuprimeCam z++	9063	1335
SC_IB427	Subaru/SuprimeCam IB427	4266	207
SC_IB464	Subaru/SuprimeCam IB464	4635	218
SC_IA484	Subaru/SuprimeCam IA484	4851	229
SC_IB505	Subaru/SuprimeCam IB505	5064	231
SC_IA527	Subaru/SuprimeCam IA527	5261	243
SC_IB574	Subaru/SuprimeCam IB574	5766	273
SC_IA624	Subaru/SuprimeCam IA624	6232	300
SC_IA679	Subaru/SuprimeCam IA679	6780	336
SC_IB709	Subaru/SuprimeCam IB709	7073	316
SC_IA738	Subaru/SuprimeCam IA738	7361	324
SC_IA767	Subaru/SuprimeCam IA767	7694	365
SC_IB827	Subaru/SuprimeCam IB827	8243	343
SC_NB711	Subaru/SuprimeCam NB711	7121	72
SC_NB816	Subaru/SuprimeCam NB816	8150	120
UVISTA_Y	VISTA/VIRCAM UltraVISTA DR4 Y	10216	923
UVISTA_J	VISTA/VIRCAM UltraVISTA DR4 J	12525	1718
UVISTA_H	VISTA/VIRCAM UltraVISTA DR4 H	16466	2905
UVISTA_Ks	VISTA/VIRCAM UltraVISTA DR4 Ks	21557	3074
UVISTA_NB118	VISTA/VIRCAM UltraVISTA DR4 NB118	11909	112
IRAC_CH1	Spitzer/IRAC ch1	35686	7443
IRAC_CH2	Spitzer/IRAC ch2	45067	10119
IRAC_CH3	Spitzer/IRAC ch3	57788	14082
IRAC_CH4	Spitzer/IRAC ch4	79958	28796
SPLASH_CH1	Spitzer/IRAC SPLASH ch1	35686	7443
SPLASH_CH2	Spitzer/IRAC SPLASH ch2	45067	10119
SPLASH_CH3	Spitzer/IRAC SPLASH ch3	57788	14082
SPLASH_CH4	Spitzer/IRAC SPLASH ch4	79958	28796

Note: see also Table 1 in Weaver et al. (2022).

describing each column. Additionally, in Sect. 6.2 we list of all the 430 columns together with their number, name, and description.

4.5   Description of The Farmer catalogue columns

```
The FARMER COSMOS2020 photometric catalog

We present here the catalog containing the photometry detected with SEP on a izYJHKs CHI-MEAN image
and extracted with The Tractor for about 1,000,000 sources in the COSMOS field within the areas of
UltraVISTA and outside the HSC bright star haloes. Suitable models are determined with izYJHKs imaging
for all detected sources, convolved with the PSF of a given band and optimised to measure flux
which is treated as a free parameter. Model parameters (radius, shape, etc.) are available upon request.
The full description of this catalog is in Weaver et al., 2022a (ApJS 258 11)

Updated 02/2022
contact: john.weaver.astro@gmail.com

##########################################################
Identification
##########################################################

Identifier
#   name = 'ID'

Right Ascension and Declination
#   name = 'ALPHA_J2000'; unit = 'deg'
#   name = 'DELTA_J2000'; unit = 'deg'

Coordinates above are based on model centroids, or SEP when models not available

Position, as determined by model centroid
#   name = 'X_MODEL'; unit = 'pixel'
#   name = 'Y_MODEL'; unit = 'pixel'
#   name = 'ERRX_MODEL'; unit = 'pixel'
#   name = 'ERRY_MODEL'; unit = 'pixel'

Position, as determined by SEP at detection, in J2000
#   name = 'ALPHA_DETECTION'; unit = 'deg'
#   name = 'DEC_DETECTION'; unit = 'deg'

Farmer model information
#   name = 'FARMER_ID'       Farmer internal source identifier ({brick}_{source})
#   name = 'GROUP_ID'        Farmer group identifier; unique within a brick
#   name = 'N_GROUP'         Farmer group occupation number
#   name = 'MODEL_FLAG'      (0: OK, 1: failed to converge, 2: drifted >0.6" from detection)
#   name = 'SOLUTION_MODEL'  The Tractor model type selected by The Farmer

Model shape information may be provided in a future release.

##########################################################
Flags
##########################################################

Flag for the bright stars and edges of the HSC images
#   name = 'FLAG_HSC'        (0:clean, 1:masked)

Flag for the bright stars and edges of the Suprime-Cam images
#   name = 'FLAG_SUPCAM'     (0:clean, 1:masked)

Flag for the UltraVISTA region
#   name = 'FLAG_UVISTA'     (0:inside, 1:outside)

Flag for the UltraVISTA ultra-deep regions
```

```
#   name = 'FLAG_UDEEP'    (0:ultra-deep, 1:deep)

Flag for the combination of FLAG_UVISTA, FLAG_HSC and FLAG_SUPCAM
#   name = 'FLAG_COMBINED' (0:clean and inside UVISTA)


############################################################
Galactic extinction at the object position
############################################################


E(B-V) values from Schlegel, Finkbeiner & Davis (1998) dust map
By default, a scaling of 0.86 is applied to the map values
to reflect the recalibration by Schlafly & Finkbeiner (2011)

#   name = 'EBV_MW'; unit = 'mag'


############################################################
Photometry
############################################################


No data convention
flux, fluxerr, mag, magerr = NaN

Negative flux convention
mag, magerr = NaN

NOTE: The photometry are not corrected for Milky Way extinction.
NOTE: The photometry are not corrected for photometric offsets derived by LePhare or EAZY
NOTE: The photometry errors are not corrected for the correlated noise in the images.


############################################################

List of bands
CFHT/MegaCam (CLAUDS): ustar, u
Subaru/HSC: g, r, i, z, y
VISTA/VIRCAM (UltraVISTA DR4): Y, J, H, Ks, NB118
Subaru/Suprime-Cam: IB427, IB464, IA484, IB505, IA527, IB574, IA624, IA679, IB709, IA738,
                    IA767, IB827, NB711, NB816
Sptizer/IRAC (Cosmic DAWN Survey): IRAC_CH1, IRAC_CH2, IRAC_CH3, IRAC_CH4

NOTE: SuprimeCam Broad bands are not measured with Farmer

Total model fluxes, flux errors, magnitudes and magnitude errors
#   name = '###_FLUX';    unit = 'uJy'
#   name = '###_FLUXERR'; unit = 'uJy'
#   name = '###_MAG';     unit = 'mag'
#   name = '###_MAGERR';  unit = 'mag'

NOTE: aperture corrections should not be applied


#   name = '###_CHISQ'  Reduced Chi2 goodness of fit statistic for source profile model
#   name = '###_DRIFT'  Distance travelled from ALPHA/DELTA_J2000 (i.e. model centroid)
#   name = '###_VALID'  Set to False where FLUX or FLUXERR not trustworthy

#   name = 'VALID_SOURCE'    Set to False when photometry failed
#   name = 'SOLUTION_MODEL'  The Tractor model type selected by The Farmer

#######################################################
Ancillary photometry

NOTE: All are matched within 0.6" radius
#######################################################

GALEX photometry (Zamojski et al. 2007) from the Capak et al. 2007 catalog
```

```
Matched identifier
#   name = 'ID_GALEX'

List of bands
  GALEX_NUV, GALEX_FUV

#   name = '###_FLUX';    unit = 'uJy'
#   name = '###_FLUXERR'; unit = 'uJy'
#   name = '###_MAG';     unit = 'mag'
#   name = '###_MAGERR';  unit = 'mag'


#####################################################

SPLASH photometry from the COSMOS2015 catalog (Laigle et al. 2016)

Matched identifier
#   name = 'ID_COSMOS2015'

List of bands
  SPLASH_CH1, SPLASH_CH2, SPLASH_CH3, SPLASH_CH4

#   name = '###_FLUX';    unit = 'uJy'
#   name = '###_FLUXERR'; unit = 'uJy'
#   name = '###_MAG';     unit = 'mag'
#   name = '###_MAGERR';  unit = 'mag'


#####################################################

HST/ACS catalog (Leauthaud et al. 2007)
selection: CLEAN == 1

Matched identifier
#   name = 'ID_ACS'

ACS photometry
#   name = 'ACS_F814W_FLUX';    unit = 'uJy'
#   name = 'ACS_F814W_FLUXERR'; unit = 'uJy'
#   name = 'ACS_F814W_MAG';     unit = 'mag'
#   name = 'ACS_F814W_MAGERR';  unit = 'mag'

ACS morphology
#   name = 'ACS_A_WORLD'; unit = 'deg'
#   name = 'ACS_B_WORLD'; unit = 'deg'
#   name = 'ACS_THETA_WORLD'; unit = 'deg'
#   name = 'ACS_FWHM_WORLD'; unit = 'deg'
#   name = 'ACS_MU_MAX'; unit = 'mag'
#   name = 'ACS_MU_CLASS'


#####################################################

Chandra COSMOS-Legacy Survey (Civano et al. 2016, Marchesi et al. 2016)

Matched identifier
#   name = 'ID_CHANDRA'


#####################################################

Corresponding Classic 2020 source

Matched identifier
#   name = 'ID_CLASSIC'


#####################################################
Le Phare photo-z and physical parameters
#####################################################
```

```
# NOTE: MW correction derived from Schlafly&Finkbeiner+2011 values assuming Allen+1976 reddening

Photometric Redshift
Derived using a method similar to Ilbert et al. (2009, 2013)
#  name = 'lp_zBEST'

   z = zPDF  if galaxy  (median of the likelihood distribution)
   z = NaN   if star, Xray source based on Chandra (Civiano program), or masked area (FLAG_HSC|FLAG_SC|FLAG_UVISTA)

Star/Galaxy Separation
See paper for details
#  name = 'lp_type'

    type=0   if galaxy
    type=1   if star (mainly 3.6 micron, and half-light radius in HSC and HST)
    type=2   if Xray source
    type=-9  if failure in the fit (most of these objects have less than 1 band)


Best fit obtained with the galaxy templates
#  name = 'lp_zPDF'          photo-z (defined as the median of the likelihood) measured using the galaxy templates
#  name = 'lp_zPDF_l68'      lower limit, 68% confidence level
#  name = 'lp_zPDF_u68'      upper limit, 68% confidence level

#  name = 'lp_zMinChi2'      photo-z (defined as the minimum of the chi2) measured using the galaxy templates
#  name = 'lp_chi2_best'     reduced chi2 (-99 if less than 3 filters) for zMinChi2

#  name = 'lp_zp_2'          second photo-z solution if a second peak is detected with P>5% in the PDF
#  name = 'lp_chi2_2'        reduced chi2 for the second photo-z solution

#  name = 'lp_NbFilt'        Number of filters used in the fit

NOTE: Every source has a redshift, regardless of the type or if it is in a masked area or not

##########################################################

Best fit obtained with the AGN templates
#  name = 'lp_zq'            photoz for the AGN library.
#  name = 'lp_chiq'          reduced chi2
#  name = 'lp_modq'          best fit template

NOTE: This value is only informative: no correction for variability is applied.

##########################################################

Best fit obtained with the STAR templates

#  name = 'lp_mods'          model for the star library
#  name = 'lp_chis'          reduced chi2

##########################################################

Corresponding mask flag if masked by FLAG_UVISTA | FLAG_HSC | FLAG_SC

#  name = 'lp_mask'

##########################################################

Physical Properties
Derived from the BC03 best-fit templates at zPDF
(Chabrier IMF; cosmo:70,0.3,0.7; BC03 tau+delayed models described in Ilbert et al. 2015).
NOTE: A value is computed for all sources, even the one in masked area or classified as star

Best fit BC03 model at zPDF
```

```
#   name = 'lp_model'                    best-fit model index
#   name = 'lp_age'                      age of best-fit template in years
#   name = 'lp_dust'                     best-fit color excess E(B-V)
#   name = 'lp_Attenuation'              best-fit dust law index

Absolute rest-frame AB magnitudes
#   name = 'lp_MFUV'            FUV galex
#   name = 'lp_MNUV'            NUV galex
#   name = 'lp_MU'             U  cfht new
#   name = 'lp_MG'             g  Subaru HSC
#   name = 'lp_MR'             r  Subaru HSC
#   name = 'lp_MI'             i  Subaru HSC
#   name = 'lp_MZ'             z  Subaru HSC
#   name = 'lp_MY'              Y VISTA
#   name = 'lp_MJ'              J VISTA
#   name = 'lp_MH'              H VISTA
#   name = 'lp_MK'              Ks VISTA

Galaxy Stellar Mass
#   name = 'lp_mass_med'        log Stellar mass from BC03 best-fit template. median of the PDF
#   name = 'lp_mass_med_min68'  lower limit, 68% confidence level
#   name = 'lp_mass_med_max68'  upper limit, 68% confidence level
#   name = 'lp_mass_best'       log Stellar mass from BC03 best-fit template. Taken at the minimum chi2

SFR and sSFR
#   name = 'lp_SFR_med'         log SFR from BC03 best-fit template. median of the PDF
#   name = 'lp_SFR_med_min68'   lower limit, 68% confidence level
#   name = 'lp_SFR_med_max68'   upper limit, 68% confidence level
#   name = 'lp_SFR_best'        log SFR from BC03 best-fit template. Taken at the minimum chi2

#   name = 'lp_sSFR_med'         log sSFR from BC03 best-fit template. median of the PDF
#   name = 'lp_sSFR_med_min68'   lower limit, 68% confidence level
#   name = 'lp_sSFR_med_max68'   upper limit, 68% confidence level
#   name = 'lp_sSFR_best'        log sSFR from BC03 best-fit template. Taken at the minimum chi2

NOTE: SFR and sSFR is computed without IR, large uncertainties with such methods

###################################################
EAZY photo-z and physical parameters
###################################################
NOTE: EAZY uses one value of Galactic extinction for all sources: E(B-V) = 0.017

Photometric redshift
Derived using the latest development version of eazy-py. See paper for details.
#   name = 'ez_z_phot'              maximum a-posteriori photometric redshift
#   name = 'ez_z_phot_chi2'         chi2 at z_phot, with z-prior
#   name = 'ez_z_phot_risk'         risk parameter from Tanaka+2018; R(ez_z_phot)
#   name = 'ez_z_min_risk'          redshift where R(z) is minimised
#   name = 'ez_min_risk'        R(ez_z_min_risk)
#   name = 'ez_z_raw_chi2'              redshift where chi2 is minimised, without priors
#   name = 'ez_raw_chi2'        chi2 at ez_z_raw_chi2

Redshift probability distribution percentiles
#   name = 'ez_z###'                025, 160, 500, 840, 975 corresponds to 2.5%, 16%, 50%, 84%, 97.5%

Fitting parameters
#   name = 'ez_nusefilt'        number of filters used for photo-z (i.e., not masked as missing data)
#   name = 'ez_lc_min'          minimum effective wavelength of valid filters, Angstrom
#   name = 'ez_lc_max'          maximum effective wavelength of valid filters, Angstrom

Best-fit stellar templates
#   name = 'ez_star_min_chi2'   chi2 of best stellar template fit (BT-SETTL models); assumes 8% systematic uncertainty
#   name = 'ez_star_teff'       effective temperature of the stellar template; unit = 'K'

#########################################################
```

```
Physical Properties
Derived from the FSPS best-fit templates (Chabrier IMF; cosmo:69.4,0.287,0.713 - WMAP9).
Dust is applied by hand using the Kriek+Conroy attenuation curve (delta=0)
Total energy absorbed by this dust screen (energy_abs) is computed, and a corresponding far-IR component is added to
the SED using the templates from Magdis+2012.

Absolute rest-frame AB magnitudes
The templates are used to perform a weighted interpolation of the rest-frame filter by refitting the templates
at ez_z_phot but with the uncertainties weighted to favour observed-frame measurements closest to the desired rest-frame band.
#  name = 'ez_restU'                 rest-frame U-band flux (units of catalog fluxes, uJy)
#  name = 'ez_restU_err'             rest-frame U-band flux uncertainty (units of catalog fluxes, uJy)
#  name = 'ez_restB'                 rest-frame B-band flux (units of catalog fluxes, uJy)
#  name = 'ez_restB_err'             rest-frame B-band flux uncertainty (units of catalog fluxes, uJy)
#  name = 'ez_restV'                 rest-frame V-band flux (units of catalog fluxes, uJy)
#  name = 'ez_restV_err'             rest-frame V-band flux uncertainty (units of catalog fluxes, uJy)
#  name = 'ez_restJ'                 rest-frame J-band flux (units of catalog fluxes, uJy)
#  name = 'ez_restJ_err'             rest-frame J-band flux uncertainty (units of catalog fluxes, uJy)

Miscellaneous properties
#  name = 'ez_dL'                    luminosity distance at z_phot; unit = 'Mpc'
#  name = 'ez_mass'                  log(mass in Msun)
#  name = 'ez_sfr'                   log(sfr in Msun/yr)
#  name = 'ez_ssfr'                  log(ssfr in 1/yr)
#  name = 'ez_Lv'                    log(V-band luminosity in Lsun)
#  name = 'ez_LIR'                   total 8-1000um luminosity in Lsun)
#  name = 'ez_energy_abs'            implied absorbed energy associated with Av; unit = 'Lsun'
#  name = 'ez_Lu'                    luminosity in U-band; unit = 'Lsun'
#  name = 'ez_Lj'                    luminosity in J-band; unit = 'Lsun'
#  name = 'ez_L1400'                 luminosity tophat filter at 1400 A; unit = 'Lsun'
#  name = 'ez_L2800'                 luminosity tophat filter at 2800 A; unit = 'Lsun'
#  name = 'ez_LHa'                   Ha line luminosity (reddened), unit = 'Lsun'
#  name = 'ez_LOIII'                 OIII line luminosity (reddened), unit = 'Lsun'
#  name = 'ez_LHb'                   Hb line luminosity (reddened), unit = 'Lsun'
#  name = 'ez_LOII'                  OII line luminosity (reddened), unit = 'Lsun'
#  name = 'ez_MLv'                   mass-to-light ratio in V-band; unit = 'Msun/Lsun'
#  name = 'ez_Av'                    extinction in V-band; unit = 'Mag'
#  name = 'ez_lwAgeV'                light-weighted age in the V-band; unit = 'Gyr'

Property percentiles
Five percentiles (025, 160, 500, 840, 975 corresponds to 2.5%, 16%, 50%, 84%, 97.5%) are computed for the following properties:
ez_mass, ez_sfr, ez_ssfr, ez_Lv, ez_LIR, ez_energy_abs, ez_Lu, ez_Lj, ez_L1400, ez_L2800, ez_L2800, ez_Ha, ez_OIII,
ez_Hb, ez_OII. All are stated in the same scaling and units as their non-percentile columns.
#  name = 'ez_XXXX_p###'
```

4.6 Masks

In the COSMOS2020 catalogues, binary flags are used to identify different regions. Four areas are indicated: the region covered by the UltraVISTA survey (FLAG_UVISTA), the region covered by 'ultra-deep' stripes within the UltraVISTA survey (FLAG_UDEEP), the area covered by bright stars in the HSC survey (FLAG_HSC) and the area covered by bright stars in the legacy Suprime-cam data (FLAG_SUPCAM). Throughout, the same convention is used: for objects with flag == 1 the object is within the masked region and should not be used. Objects with flag == 0 are outside the masked region. These different masks are summarized in Table 5 and graphically in Figure 2. Also listed are the ds9[9] region files which are being made available with this release.

---

[9]sites.google.com/cfa.harvard.edu/saoimageds9/home

Table 5: A summary of the flags provided in the catalogue together with their associated region files.

Mask name	Area (deg^2)	Region file
FLAG_HSC	2.75	MASK_HSC-stars_griz.reg
FLAG_UVISTA	1.792	MASK_UVISTA.reg
FLAG_UDEEP	1.054	MASK_UDEEP.reg
FLAG_SUPCAM	1.918	MASK_SUPCAM.reg
FLAG_COMBINED	1.27	(all of the above except UDEEP)
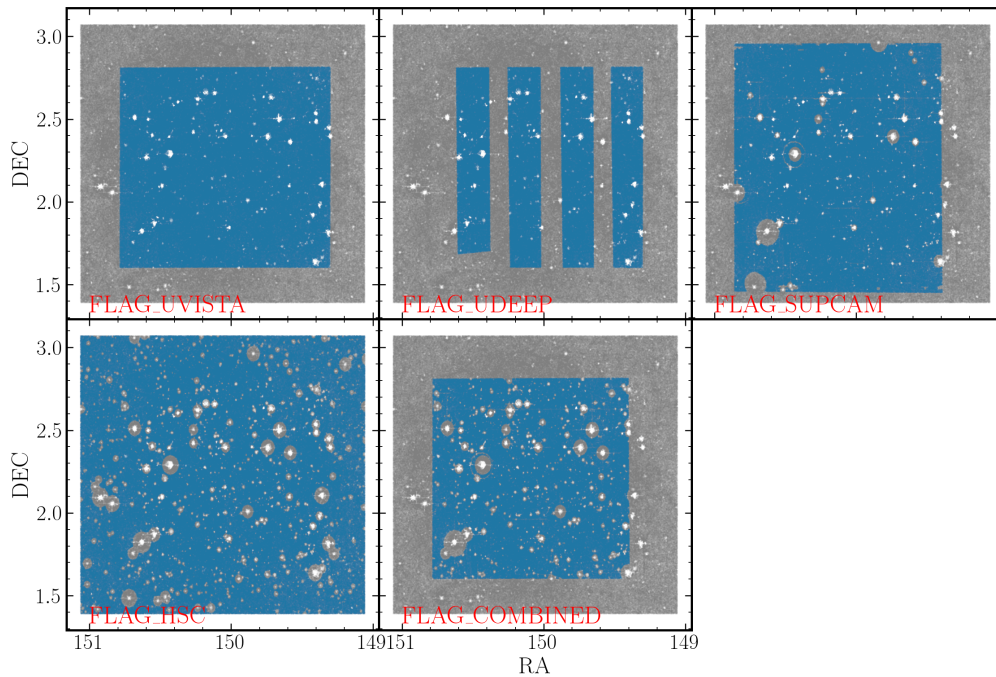
Figure 2: An illustration of the areas covered by each of the five different mask types present in the catalogue. Blue regions show the zones covered by the masks.

4.7 Redshift probability distributions

For each source, in both catalogues, we provide the redshift probability distributions or $p(z)$. These are stored as fits files.

The $p(z)$ results from `LePhare` are recorded as the likelihood at a given redshift spanning a baseline from $z = 0$ to 10 sampling in 1001 points of equal-z.

Slightly differently, the $p(z)$ results from `EAZY` are stored instead as 50 samplings of the cumulative redshift probability distribution or $cdf(z)$, equally spaced according to multiples of the standard deviation of a Gaussian distribution. As such, the $p(z)$ can be easily reconstructed from the relatively more compact $cdf(z)$ data without a significant loss of precision. Alternatively, users may find it advantageous to simply assess the probability of a source being in a certain redshift range by taking the difference in the $cdf(z)$ at two z points, equivalent to integrating the $p(z)$ but with much less computational effort. A script is provided to help users access and use this format.

4.8 Other products

Before photometric redshift measurements are made from photometric data, a series of corrections are applied to each object. These include correction of Milky Way extinction based on the value of $E(B - V)$ derived from dust maps and the application of a series of aperture offsets to bring individual colours to total photometry. At the release website, CLASSIC catalogue, we provide a `Python` program to compute this offset.

5 Acknowledgements

A full list of acknowledgements for the data sources used in this catalogue, together with their associated bibliographic references, can be found in Weaver et al. (2022).

6 Appendices

6.1 Complete list of Classic catalogue columns

Not applicable because DR4.1.1 does not include the CLASSIC catalogue (see DR4.1 for that).

6.2 Complete list of The Farmer catalogue columns

The following is a list of number, name, description and unit for all the columns in THE FARMER.

```
No. | Column name       | Column description                                          | Column unit
-------------------------------------------------------------------------------------------------------
  1 | ID                | ID (specifically ID_FARMER, as this is the Farmer catalogue) |
  2 | ALPHA_J2000       | Right ascension (J2000) of model, or of SEP when model is not avail. | deg
  3 | DELTA_J2000       | Declination (J2000) of model, or of SEP when model is not available | deg
  4 | X_MODEL           | Object model position along X, with the scale being 0.15"/px | pix
```

```
 5 | Y_MODEL            | Object model position along Y, with the scale being 0.15"/px  | pix
 6 | ERRX_MODEL         | Uncertainty on object model position along X                 | pix
 7 | ERRY_MODEL         | Uncertainty on object model position along Y                 | pix
 8 | ALPHA_DETECTION    | Right ascension (J2000) of object as determined by SEP at detection | deg
 9 | DELTA_DETECTION    | Declination (J2000) of object as determined by SEP at detection | deg
10 | FARMER_ID          | Farmer internal source identifier ({brick}_{source})         |
11 | GROUP_ID           | Farmer group identifier; unique within a brick               |
12 | N_GROUP            | Farmer group occupation number                               |
13 | MODEL_FLAG         | Flag (0: OK, 1: failed to converge, 2: drifted >0.6" from detection) |
14 | SOLUTION_MODEL     | The Tractor model type selected by The Farmer                |
15 | FLAG_HSC           | Flag indicating quality of HSC imaging (0:clean, 1:masked)   |
16 | FLAG_SUPCAM        | Flag indicating quality of Suprime-Cam imaging (0:clean, 1:masked) |
17 | FLAG_UDEEP         | Flag for the UltraVISTA ultra-deep regions (0:ultra-deep, 1:deep) |
18 | FLAG_UVISTA        | Flag for the UltraVISTA region (0:inside, 1:outside)         |
19 | FLAG_COMBINED      | Comb. FLAG_UVISTA, FLAG_HSC, FLAG_SUPCAM (0:clean and inside UVISTA) |
20 | EBV_MW             | Galactic reddening E(B-V) (Schlegel+1998, Schlafly&Finkbeiner 2011) |
21 | CFHT_u_FLUX        | CFHT_u flux density                                          | uJy
22 | CFHT_u_FLUXERR     | CFHT_u flux density error                                    | uJy
23 | CFHT_u_MAG         | CFHT_u AB magnitude                                          | mag
24 | CFHT_u_MAGERR      | CFHT_u AB magnitude error                                    | mag
25 | CFHT_u_CHISQ       | CFHT_u reduced Chi2 goodness of fit stat for source prof model |
26 | CFHT_u_DRIFT       | CFHT_u distance travelled from RA,Dec model centroid         | arcsec
27 | CFHT_u_VALID       | CFHT_u flag=False if FLUX/MAG or its error is not trustworthy |
28 | CFHT_ustar_FLUX    | CFHT_ustar flux density                                      | uJy
29 | CFHT_ustar_FLUXERR | CFHT_ustar flux density error                                | uJy
30 | CFHT_ustar_MAG     | CFHT_ustar AB magnitude                                      | mag
31 | CFHT_ustar_MAGERR  | CFHT_ustar AB magnitude error                                | mag
32 | CFHT_ustar_CHISQ   | CFHT_ustar reduced Chi2 goodness of fit stat for source prof model |
33 | CFHT_ustar_DRIFT   | CFHT_ustar distance travelled from RA,Dec model centroid     | arcsec
34 | CFHT_ustar_VALID   | CFHT_ustar flag=False if FLUX/MAG or its error is not trustworthy |
35 | HSC_g_FLUX         | HSC_g flux density                                          | uJy
36 | HSC_g_FLUXERR      | HSC_g flux density error                                    | uJy
37 | HSC_g_MAG          | HSC_g AB magnitude                                          | mag
38 | HSC_g_MAGERR       | HSC_g AB magnitude error                                    | mag
39 | HSC_g_CHISQ        | HSC_g reduced Chi2 goodness of fit stat for source prof model |
40 | HSC_g_DRIFT        | HSC_g distance travelled from RA,Dec model centroid         | arcsec
41 | HSC_g_VALID        | HSC_g flag=False if FLUX/MAG or its error is not trustworthy |
42 | HSC_r_FLUX         | HSC_r flux density                                          | uJy
43 | HSC_r_FLUXERR      | HSC_r flux density error                                    | uJy
44 | HSC_r_MAG          | HSC_r AB magnitude                                          | mag
45 | HSC_r_MAGERR       | HSC_r AB magnitude error                                    | mag
46 | HSC_r_CHISQ        | HSC_r reduced Chi2 goodness of fit stat for source prof model |
47 | HSC_r_DRIFT        | HSC_r distance travelled from RA,Dec model centroid         | arcsec
48 | HSC_r_VALID        | HSC_r flag=False if FLUX/MAG or its error is not trustworthy |
49 | HSC_i_FLUX         | HSC_i flux density                                          | uJy
50 | HSC_i_FLUXERR      | HSC_i flux density error                                    | uJy
51 | HSC_i_MAG          | HSC_i AB magnitude                                          | mag
52 | HSC_i_MAGERR       | HSC_i AB magnitude error                                    | mag
53 | HSC_i_CHISQ        | HSC_i reduced Chi2 goodness of fit stat for source prof model |
54 | HSC_i_DRIFT        | HSC_i distance travelled from RA,Dec model centroid         | arcsec
55 | HSC_i_VALID        | HSC_i flag=False if FLUX/MAG or its error is not trustworthy |
56 | HSC_z_FLUX         | HSC_z flux density                                          | uJy
57 | HSC_z_FLUXERR      | HSC_z flux density error                                    | uJy
58 | HSC_z_MAG          | HSC_z AB magnitude                                          | mag
59 | HSC_z_MAGERR       | HSC_z AB magnitude error                                    | mag
60 | HSC_z_CHISQ        | HSC_z reduced Chi2 goodness of fit stat for source prof model |
61 | HSC_z_DRIFT        | HSC_z distance travelled from RA,Dec model centroid         | arcsec
62 | HSC_z_VALID        | HSC_z flag=False if FLUX/MAG or its error is not trustworthy |
63 | HSC_y_FLUX         | HSC_y flux density                                          | uJy
64 | HSC_y_FLUXERR      | HSC_y flux density error                                    | uJy
65 | HSC_y_MAG          | HSC_y AB magnitude                                          | mag
66 | HSC_y_MAGERR       | HSC_y AB magnitude error                                    | mag
67 | HSC_y_CHISQ        | HSC_y reduced Chi2 goodness of fit stat for source prof model |
68 | HSC_y_DRIFT        | HSC_y distance travelled from RA,Dec model centroid         | arcsec
69 | HSC_y_VALID        | HSC_y flag=False if FLUX/MAG or its error is not trustworthy |
```

```
 70 | UVISTA_Y_FLUX        | UVISTA_Y flux density                                  | uJy
 71 | UVISTA_Y_FLUXERR     | UVISTA_Y flux density error                            | uJy
 72 | UVISTA_Y_MAG         | UVISTA_Y AB magnitude                                  | mag
 73 | UVISTA_Y_MAGERR      | UVISTA_Y AB magnitude error                            | mag
 74 | UVISTA_Y_CHISQ       | UVISTA_Y reduced Chi2 goodness of fit stat for source prof model |
 75 | UVISTA_Y_DRIFT       | UVISTA_Y distance travelled from RA,Dec model centroid | arcsec
 76 | UVISTA_Y_VALID       | UVISTA_Y flag=False if FLUX/MAG or its error is not trustworthy |
 77 | UVISTA_J_FLUX        | UVISTA_J flux density                                  | uJy
 78 | UVISTA_J_FLUXERR     | UVISTA_J flux density error                            | uJy
 79 | UVISTA_J_MAG         | UVISTA_J AB magnitude                                  | mag
 80 | UVISTA_J_MAGERR      | UVISTA_J AB magnitude error                            | mag
 81 | UVISTA_J_CHISQ       | UVISTA_J reduced Chi2 goodness of fit stat for source prof model |
 82 | UVISTA_J_DRIFT       | UVISTA_J distance travelled from RA,Dec model centroid | arcsec
 83 | UVISTA_J_VALID       | UVISTA_J flag=False if FLUX/MAG or its error is not trustworthy |
 84 | UVISTA_H_FLUX        | UVISTA_H flux density                                  | uJy
 85 | UVISTA_H_FLUXERR     | UVISTA_H flux density error                            | uJy
 86 | UVISTA_H_MAG         | UVISTA_H AB magnitude                                  | mag
 87 | UVISTA_H_MAGERR      | UVISTA_H AB magnitude error                            | mag
 88 | UVISTA_H_CHISQ       | UVISTA_H reduced Chi2 goodness of fit stat for source prof model |
 89 | UVISTA_H_DRIFT       | UVISTA_H distance travelled from RA,Dec model centroid | arcsec
 90 | UVISTA_H_VALID       | UVISTA_H flag=False if FLUX/MAG or its error is not trustworthy |
 91 | UVISTA_Ks_FLUX       | UVISTA_Ks flux density                                 | uJy
 92 | UVISTA_Ks_FLUXERR    | UVISTA_Ks flux density error                           | uJy
 93 | UVISTA_Ks_MAG        | UVISTA_Ks AB magnitude                                 | mag
 94 | UVISTA_Ks_MAGERR     | UVISTA_Ks AB magnitude error                           | mag
 95 | UVISTA_Ks_CHISQ      | UVISTA_Ks reduced Chi2 goodness of fit stat for source prof model |
 96 | UVISTA_Ks_DRIFT      | UVISTA_Ks distance travelled from RA,Dec model centroid | arcsec
 97 | UVISTA_Ks_VALID      | UVISTA_Ks flag=False if FLUX/MAG or its error is not trustworthy |
 98 | UVISTA_NB118_FLUX    | UVISTA_NB118 flux density                              | uJy
 99 | UVISTA_NB118_FLUXERR | UVISTA_NB118 flux density error                        | uJy
100 | UVISTA_NB118_MAG     | UVISTA_NB118 AB magnitude                              | mag
101 | UVISTA_NB118_MAGERR  | UVISTA_NB118 AB magnitude error                        | mag
102 | UVISTA_NB118_CHISQ   | UVISTA_NB118 reduced Chi2 goodness of fit stat for source prof model |
103 | UVISTA_NB118_DRIFT   | UVISTA_NB118 distance travelled from RA,Dec model centroid | arcsec
104 | UVISTA_NB118_VALID   | UVISTA_NB118 flag=False if FLUX/MAG or its error is not trustworthy |
105 | SC_IB427_FLUX        | SC_IB427 flux density                                  | uJy
106 | SC_IB427_FLUXERR     | SC_IB427 flux density error                            | uJy
107 | SC_IB427_MAG         | SC_IB427 AB magnitude                                  | mag
108 | SC_IB427_MAGERR      | SC_IB427 AB magnitude error                            | mag
109 | SC_IB427_CHISQ       | SC_IB427 reduced Chi2 goodness of fit stat for source prof model |
110 | SC_IB427_DRIFT       | SC_IB427 distance travelled from RA,Dec model centroid | arcsec
111 | SC_IB427_VALID       | SC_IB427 flag=False if FLUX/MAG or its error is not trustworthy |
112 | SC_IB464_FLUX        | SC_IB464 flux density                                  | uJy
113 | SC_IB464_FLUXERR     | SC_IB464 flux density error                            | uJy
114 | SC_IB464_MAG         | SC_IB464 AB magnitude                                  | mag
115 | SC_IB464_MAGERR      | SC_IB464 AB magnitude error                            | mag
116 | SC_IB464_CHISQ       | SC_IB464 reduced Chi2 goodness of fit stat for source prof model |
117 | SC_IB464_DRIFT       | SC_IB464 distance travelled from RA,Dec model centroid | arcsec
118 | SC_IB464_VALID       | SC_IB464 flag=False if FLUX/MAG or its error is not trustworthy |
119 | SC_IA484_FLUX        | SC_IA484 flux density                                  | uJy
120 | SC_IA484_FLUXERR     | SC_IA484 flux density error                            | uJy
121 | SC_IA484_MAG         | SC_IA484 AB magnitude                                  | mag
122 | SC_IA484_MAGERR      | SC_IA484 AB magnitude error                            | mag
123 | SC_IA484_CHISQ       | SC_IA484 reduced Chi2 goodness of fit stat for source prof model |
124 | SC_IA484_DRIFT       | SC_IA484 distance travelled from RA,Dec model centroid | arcsec
125 | SC_IA484_VALID       | SC_IA484 flag=False if FLUX/MAG or its error is not trustworthy |
126 | SC_IB505_FLUX        | SC_IB505 flux density                                  | uJy
127 | SC_IB505_FLUXERR     | SC_IB505 flux density error                            | uJy
128 | SC_IB505_MAG         | SC_IB505 AB magnitude                                  | mag
129 | SC_IB505_MAGERR      | SC_IB505 AB magnitude error                            | mag
130 | SC_IB505_CHISQ       | SC_IB505 reduced Chi2 goodness of fit stat for source prof model |
131 | SC_IB505_DRIFT       | SC_IB505 distance travelled from RA,Dec model centroid | arcsec
132 | SC_IB505_VALID       | SC_IB505 flag=False if FLUX/MAG or its error is not trustworthy |
133 | SC_IA527_FLUX        | SC_IA527 flux density                                  | uJy
134 | SC_IA527_FLUXERR     | SC_IA527 flux density error                            | uJy
```

```
135 | SC_IA527_MAG        | SC_IA527 AB magnitude                                  | mag
136 | SC_IA527_MAGERR     | SC_IA527 AB magnitude error                            | mag
137 | SC_IA527_CHISQ      | SC_IA527 reduced Chi2 goodness of fit stat for source prof model  |
138 | SC_IA527_DRIFT      | SC_IA527 distance travelled from RA,Dec model centroid | arcsec
139 | SC_IA527_VALID      | SC_IA527 flag=False if FLUX/MAG or its error is not trustworthy  |
140 | SC_IB574_FLUX       | SC_IB574 flux density                                  | uJy
141 | SC_IB574_FLUXERR    | SC_IB574 flux density error                            | uJy
142 | SC_IB574_MAG        | SC_IB574 AB magnitude                                  | mag
143 | SC_IB574_MAGERR     | SC_IB574 AB magnitude error                            | mag
144 | SC_IB574_CHISQ      | SC_IB574 reduced Chi2 goodness of fit stat for source prof model  |
145 | SC_IB574_DRIFT      | SC_IB574 distance travelled from RA,Dec model centroid | arcsec
146 | SC_IB574_VALID      | SC_IB574 flag=False if FLUX/MAG or its error is not trustworthy  |
147 | SC_IA624_FLUX       | SC_IA624 flux density                                  | uJy
148 | SC_IA624_FLUXERR    | SC_IA624 flux density error                            | uJy
149 | SC_IA624_MAG        | SC_IA624 AB magnitude                                  | mag
150 | SC_IA624_MAGERR     | SC_IA624 AB magnitude error                            | mag
151 | SC_IA624_CHISQ      | SC_IA624 reduced Chi2 goodness of fit stat for source prof model  |
152 | SC_IA624_DRIFT      | SC_IA624 distance travelled from RA,Dec model centroid | arcsec
153 | SC_IA624_VALID      | SC_IA624 flag=False if FLUX/MAG or its error is not trustworthy  |
154 | SC_IA679_FLUX       | SC_IA679 flux density                                  | uJy
155 | SC_IA679_FLUXERR    | SC_IA679 flux density error                            | uJy
156 | SC_IA679_MAG        | SC_IA679 AB magnitude                                  | mag
157 | SC_IA679_MAGERR     | SC_IA679 AB magnitude error                            | mag
158 | SC_IA679_CHISQ      | SC_IA679 reduced Chi2 goodness of fit stat for source prof model  |
159 | SC_IA679_DRIFT      | SC_IA679 distance travelled from RA,Dec model centroid | arcsec
160 | SC_IA679_VALID      | SC_IA679 flag=False if FLUX/MAG or its error is not trustworthy  |
161 | SC_IB709_FLUX       | SC_IB709 flux density                                  | uJy
162 | SC_IB709_FLUXERR    | SC_IB709 flux density error                            | uJy
163 | SC_IB709_MAG        | SC_IB709 AB magnitude                                  | mag
164 | SC_IB709_MAGERR     | SC_IB709 AB magnitude error                            | mag
165 | SC_IB709_CHISQ      | SC_IB709 reduced Chi2 goodness of fit stat for source prof model  |
166 | SC_IB709_DRIFT      | SC_IB709 distance travelled from RA,Dec model centroid | arcsec
167 | SC_IB709_VALID      | SC_IB709 flag=False if FLUX/MAG or its error is not trustworthy  |
168 | SC_IA738_FLUX       | SC_IA738 flux density                                  | uJy
169 | SC_IA738_FLUXERR    | SC_IA738 flux density error                            | uJy
170 | SC_IA738_MAG        | SC_IA738 AB magnitude                                  | mag
171 | SC_IA738_MAGERR     | SC_IA738 AB magnitude error                            | mag
172 | SC_IA738_CHISQ      | SC_IA738 reduced Chi2 goodness of fit stat for source prof model  |
173 | SC_IA738_DRIFT      | SC_IA738 distance travelled from RA,Dec model centroid | arcsec
174 | SC_IA738_VALID      | SC_IA738 flag=False if FLUX/MAG or its error is not trustworthy  |
175 | SC_IA767_FLUX       | SC_IA767 flux density                                  | uJy
176 | SC_IA767_FLUXERR    | SC_IA767 flux density error                            | uJy
177 | SC_IA767_MAG        | SC_IA767 AB magnitude                                  | mag
178 | SC_IA767_MAGERR     | SC_IA767 AB magnitude error                            | mag
179 | SC_IA767_CHISQ      | SC_IA767 reduced Chi2 goodness of fit stat for source prof model  |
180 | SC_IA767_DRIFT      | SC_IA767 distance travelled from RA,Dec model centroid | arcsec
181 | SC_IA767_VALID      | SC_IA767 flag=False if FLUX/MAG or its error is not trustworthy  |
182 | SC_IB827_FLUX       | SC_IB827 flux density                                  | uJy
183 | SC_IB827_FLUXERR    | SC_IB827 flux density error                            | uJy
184 | SC_IB827_MAG        | SC_IB827 AB magnitude                                  | mag
185 | SC_IB827_MAGERR     | SC_IB827 AB magnitude error                            | mag
186 | SC_IB827_CHISQ      | SC_IB827 reduced Chi2 goodness of fit stat for source prof model  |
187 | SC_IB827_DRIFT      | SC_IB827 distance travelled from RA,Dec model centroid | arcsec
188 | SC_IB827_VALID      | SC_IB827 flag=False if FLUX/MAG or its error is not trustworthy  |
189 | SC_NB711_FLUX       | SC_NB711 flux density                                  | uJy
190 | SC_NB711_FLUXERR    | SC_NB711 flux density error                            | uJy
191 | SC_NB711_MAG        | SC_NB711 AB magnitude                                  | mag
192 | SC_NB711_MAGERR     | SC_NB711 AB magnitude error                            | mag
193 | SC_NB711_CHISQ      | SC_NB711 reduced Chi2 goodness of fit stat for source prof model  |
194 | SC_NB711_DRIFT      | SC_NB711 distance travelled from RA,Dec model centroid | arcsec
195 | SC_NB711_VALID      | SC_NB711 flag=False if FLUX/MAG or its error is not trustworthy  |
196 | SC_NB816_FLUX       | SC_NB816 flux density                                  | uJy
197 | SC_NB816_FLUXERR    | SC_NB816 flux density error                            | uJy
198 | SC_NB816_MAG        | SC_NB816 AB magnitude                                  | mag
199 | SC_NB816_MAGERR     | SC_NB816 AB magnitude error                            | mag
```

```
200 | SC_NB816_CHISQ      | SC_NB816 reduced Chi2 goodness of fit stat for source prof model  |
201 | SC_NB816_DRIFT      | SC_NB816 distance travelled from RA,Dec model centroid            | arcsec
202 | SC_NB816_VALID      | SC_NB816 flag=False if FLUX/MAG or its error is not trustworthy   |
203 | IRAC_CH1_FLUX       | IRAC_CH1 flux density                                            | uJy
204 | IRAC_CH1_FLUXERR    | IRAC_CH1 flux density error                                      | uJy
205 | IRAC_CH1_MAG        | IRAC_CH1 AB magnitude                                            | mag
206 | IRAC_CH1_MAGERR     | IRAC_CH1 AB magnitude error                                      | mag
207 | IRAC_CH1_CHISQ      | IRAC_CH1 reduced Chi2 goodness of fit stat for source prof model  |
208 | IRAC_CH1_DRIFT      | IRAC_CH1 distance travelled from RA,Dec model centroid            | arcsec
209 | IRAC_CH1_VALID      | IRAC_CH1 flag=False if FLUX/MAG or its error is not trustworthy   |
210 | IRAC_CH2_FLUX       | IRAC_CH2 flux density                                            | uJy
211 | IRAC_CH2_FLUXERR    | IRAC_CH2 flux density error                                      | uJy
212 | IRAC_CH2_MAG        | IRAC_CH2 AB magnitude                                            | mag
213 | IRAC_CH2_MAGERR     | IRAC_CH2 AB magnitude error                                      | mag
214 | IRAC_CH2_CHISQ      | IRAC_CH2 reduced Chi2 goodness of fit stat for source prof model  |
215 | IRAC_CH2_DRIFT      | IRAC_CH2 distance travelled from RA,Dec model centroid            | arcsec
216 | IRAC_CH2_VALID      | IRAC_CH2 flag=False if FLUX/MAG or its error is not trustworthy   |
217 | IRAC_CH3_FLUX       | IRAC_CH3 flux density                                            | uJy
218 | IRAC_CH3_FLUXERR    | IRAC_CH3 flux density error                                      | uJy
219 | IRAC_CH3_MAG        | IRAC_CH3 AB magnitude                                            | mag
220 | IRAC_CH3_MAGERR     | IRAC_CH3 AB magnitude error                                      | mag
221 | IRAC_CH3_CHISQ      | IRAC_CH3 reduced Chi2 goodness of fit stat for source prof model  |
222 | IRAC_CH3_DRIFT      | IRAC_CH3 distance travelled from RA,Dec model centroid            | arcsec
223 | IRAC_CH3_VALID      | IRAC_CH3 flag=False if FLUX/MAG or its error is not trustworthy   |
224 | IRAC_CH4_FLUX       | IRAC_CH4 flux density                                            | uJy
225 | IRAC_CH4_FLUXERR    | IRAC_CH4 flux density error                                      | uJy
226 | IRAC_CH4_MAG        | IRAC_CH4 AB magnitude                                            | mag
227 | IRAC_CH4_MAGERR     | IRAC_CH4 AB magnitude error                                      | mag
228 | IRAC_CH4_CHISQ      | IRAC_CH4 reduced Chi2 goodness of fit stat for source prof model  |
229 | IRAC_CH4_DRIFT      | IRAC_CH4 distance travelled from RA,Dec model centroid            | arcsec
230 | IRAC_CH4_VALID      | IRAC_CH4 flag=False if FLUX/MAG or its error is not trustworthy   |
231 | ID_GALEX            | ID in GALEX cat. (Zamojski+2007, Capak+2007), crossm. with 0.6" rad. |
232 | GALEX_NUV_FLUX      | GALEX_NUV flux density                                           | uJy
233 | GALEX_NUV_FLUXERR   | GALEX_NUV flux density error                                     | uJy
234 | GALEX_NUV_MAG       | GALEX_NUV AB magnitude                                           | mag
235 | GALEX_NUV_MAGERR    | GALEX_NUV AB magnitude error                                     | mag
236 | GALEX_FUV_FLUX      | GALEX_FUV flux density                                           | uJy
237 | GALEX_FUV_FLUXERR   | GALEX_FUV flux density error                                     | uJy
238 | GALEX_FUV_MAG       | GALEX_FUV AB magnitude                                           | mag
239 | GALEX_FUV_MAGERR    | GALEX_FUV AB magnitude error                                     | mag
240 | ID_COSMOS2015       | ID in COSMOS2015 cat. (Laigle+2016), crossmatched with 0.6" radius |
241 | SPLASH_CH1_FLUX     | SPLASH_CH1 flux density                                          | uJy
242 | SPLASH_CH1_FLUXERR  | SPLASH_CH1 flux density error                                    | uJy
243 | SPLASH_CH1_MAG      | SPLASH_CH1 AB magnitude                                          | mag
244 | SPLASH_CH1_MAGERR   | SPLASH_CH1 AB magnitude error                                    | mag
245 | SPLASH_CH2_FLUX     | SPLASH_CH2 flux density                                          | uJy
246 | SPLASH_CH2_FLUXERR  | SPLASH_CH2 flux density error                                    | uJy
247 | SPLASH_CH2_MAG      | SPLASH_CH2 AB magnitude                                          | mag
248 | SPLASH_CH2_MAGERR   | SPLASH_CH2 AB magnitude error                                    | mag
249 | SPLASH_CH3_FLUX     | SPLASH_CH3 flux density                                          | uJy
250 | SPLASH_CH3_FLUXERR  | SPLASH_CH3 flux density error                                    | uJy
251 | SPLASH_CH3_MAG      | SPLASH_CH3 AB magnitude                                          | mag
252 | SPLASH_CH3_MAGERR   | SPLASH_CH3 AB magnitude error                                    | mag
253 | SPLASH_CH4_FLUX     | SPLASH_CH4 flux density                                          | uJy
254 | SPLASH_CH4_FLUXERR  | SPLASH_CH4 flux density error                                    | uJy
255 | SPLASH_CH4_MAG      | SPLASH_CH4 AB magnitude                                          | mag
256 | SPLASH_CH4_MAGERR   | SPLASH_CH4 AB magnitude error                                    | mag
257 | ID_ACS              | ID in HST ACS F814W cat. (Leauthaud+2007), crossm. with 0.6" radius |
258 | ACS_F814W_MAG       | ACS_F814W AB magnitude                                           | mag
259 | ACS_F814W_MAGERR    | ACS_F814W AB magnitude error                                     | mag
260 | ACS_F814W_FLUX      | ACS_F814W flux density                                           | uJy
261 | ACS_F814W_FLUXERR   | ACS_F814W flux density error                                     | uJy
262 | ACS_A_WORLD         | ACS F814W semi-major axis length                                | deg
263 | ACS_B_WORLD         | ACS F814W semi-minor axis length                                | deg
264 | ACS_THETA_WORLD     | ACS F814W angle; to get PA measured from N through E, add/subtr. 90 | deg
```

```
265 | ACS_FWHM_WORLD      | ACS F814W FWHM assuming a gaussian core                        | deg
266 | ACS_MU_MAX          | ACS F814W peak surface brightness above background            |
267 | ACS_MU_CLASS        | ACS F814W star/galaxy classifier: 1=galaxy, 2=star, 3=fake detection |
268 | ID_CHANDRA          | ID in Chandra cat. (Civano+2016, Marchesi+2016), crossm. w. 0.6" rad |
269 | ID_CLASSIC          | ID in the Classic catalogue, crossmatched with 0.6" radius    |
270 | lp_zBEST            | LePhare photo-z (=lp_zPDF if galaxy, NaN if X-ray source or masked) |
271 | lp_type             | LePhare type (0: galaxy, 1: star, 2: Xray sour., -9: failure in fit) |
272 | lp_zPDF             | LePhare photo-z using the galaxy templ., median of likelihood distr. |
273 | lp_zPDF_l68         | LePhare photo-z lower limit, 68% confidence level (galaxy templates) |
274 | lp_zPDF_u68         | LePhare photo-z upper limit, 68% confidence level (galaxy templates) |
275 | lp_zMinChi2         | LePhare photo-z using the galaxy templates, minimum chi2      |
276 | lp_chi2_best        | LePhare reduced chi2 for lp_zMinChi2 (NaN if less than 3 filters) |
277 | lp_zp_2             | LePhare 2nd photo-z solution if a 2nd peak detected w. P>5% in PDF |
278 | lp_chi2_2           | LePhare reduced chi2 for the second photo-z solution         |
279 | lp_NbFilt           | LePhare number of filters used in the fit                    |
280 | lp_zq               | LePhare photo-z for the AGN library                          |
281 | lp_chiq             | LePhare reduced chi2 for photo-z for the AGN library         |
282 | lp_modq             | LePhare best fit template number in the AGN library          |
283 | lp_mods             | LePhare best fit template number in the star library         |
284 | lp_chis             | LePhare reduced chi2 for the best fit with the star library  |
285 | lp_mask             | LePhare mask flag (0: in UVISTA and in clean part of HSC and SUPCAM) |
286 | lp_model            | LePhare BC03 best fit template number                        |
287 | lp_age              | LePhare BC03 age of best fit template at zPDF                | yr
288 | lp_dust             | LePhare BC03 colour excess E(B-V) of best fit template at zPDF |
289 | lp_Attenuation      | LePhare BC03 best-fit dust law number at zPDF                |
290 | lp_MFUV             | LePhare BC03 absolute rest-frame AB mag in GALEX FUV band at zPDF | mag
291 | lp_MNUV             | LePhare BC03 absolute rest-frame AB mag in GALEX NUV band at zPDF | mag
292 | lp_MU               | LePhare BC03 absolute rest-frame AB mag in CFHT u* band at zPDF | mag
293 | lp_MG               | LePhare BC03 absolute rest-frame AB mag in Subaru/HSC g band at zPDF | mag
294 | lp_MR               | LePhare BC03 absolute rest-frame AB mag in Subaru/HSC r band at zPDF | mag
295 | lp_MI               | LePhare BC03 absolute rest-frame AB mag in Subaru/HSC i band at zPDF | mag
296 | lp_MZ               | LePhare BC03 absolute rest-frame AB mag in Subaru/HSC z band at zPDF | mag
297 | lp_MY               | LePhare BC03 absolute rest-frame AB mag in VISTA Y band at zPDF | mag
298 | lp_MJ               | LePhare BC03 absolute rest-frame AB mag in VISTA J band at zPDF | mag
299 | lp_MH               | LePhare BC03 absolute rest-frame AB mag in VISTA H band at zPDF | mag
300 | lp_MK               | LePhare BC03 absolute rest-frame AB mag in VISTA Ks band at zPDF | mag
301 | lp_mass_med         | LePhare BC03 log stellar mass at zPDF                        | log(solMass)
302 | lp_mass_med_min68   | LePhare BC03 log stellar mass at zPDF, lower limit, 68% conf. level | log(solMass)
303 | lp_mass_med_max68   | LePhare BC03 log stellar mass at zPDF, upper limit, 68% conf. level | log(solMass)
304 | lp_mass_best        | LePhare BC03 log stellar mass at zMinChi2                    | log(solMass)
305 | lp_SFR_med          | LePhare BC03 log SFR at zPDF                                 | log(solMass/yr)
306 | lp_SFR_med_min68    | LePhare BC03 log SFR at zPDF, lower limit, 68% confidence level | log(solMass/yr)
307 | lp_SFR_med_max68    | LePhare BC03 log SFR at zPDF, upper limit, 68% confidence level | log(solMass/yr)
308 | lp_SFR_best         | LePhare BC03 log SFR at zMinChi2                             | log(solMass/yr)
309 | lp_sSFR_med         | LePhare BC03 log sSFR at zPDF                                | log(yr**(-1))
310 | lp_sSFR_med_min68   | LePhare BC03 log sSFR at zPDF, lower limit, 68% confidence level | log(yr**(-1))
311 | lp_sSFR_med_max68   | LePhare BC03 log sSFR at zPDF, upper limit, 68% confidence level | log(yr**(-1))
312 | lp_sSFR_best        | LePhare BC03 log sSFR at zMinChi2                            | log(yr**(-1))
313 | ez_z_phot           | EAZY maximum a-posteriori photo-z                           |
314 | ez_z_phot_chi2      | EAZY chi2 at ez_z_phot, with z-prior                        |
315 | ez_z_phot_risk      | EAZY risk parameter (Tanaka+2018) at ez_z_phot, R(ez_z_phot) |
316 | ez_z_min_risk       | EAZY photo-z where risk parameter R(z) is minimised         |
317 | ez_min_risk         | EAZY risk parameter at ez_z_min_risk, R(ez_z_min_risk)      |
318 | ez_z_raw_chi2       | EAZY photo-z where chi2 is minimised, without priors        |
319 | ez_raw_chi2         | EAZY chi2 at ez_z_raw_chi2                                  |
320 | ez_z025             | EAZY  2.5% percentile of photo-z                            |
321 | ez_z160             | EAZY 16.0% percentile of photo-z                            |
322 | ez_z500             | EAZY 50.0% percentile of photo-z                            |
323 | ez_z840             | EAZY 84.0% percentile of photo-z                            |
324 | ez_z975             | EAZY 97.5% percentile of photo-z                            |
325 | ez_nusefilt         | EAZY no. of filters used for photo-z (only filters w/o missing data) |
326 | ez_lc_min           | EAZY minimum effective wavelength of valid filters          | Angstrom
327 | ez_lc_max           | EAZY minimum effective wavelength of valid filters          | Angstrom
328 | ez_star_min_chi2    | EAZY chi2 best stellar template fit (BT-SETTL models) as, 8% sys unc |
329 | ez_star_teff        | EAZY effective temperature of the stellar template          | K
```

```
330 | ez_restU            | EAZY rest-frame U-band flux density                           | uJy
331 | ez_restU_err        | EAZY rest-frame U-band flux density uncertainty               | uJy
332 | ez_restB            | EAZY rest-frame B-band flux density                           | uJy
333 | ez_restB_err        | EAZY rest-frame B-band flux density uncertainty               | uJy
334 | ez_restV            | EAZY rest-frame V-band flux density                           | uJy
335 | ez_restV_err        | EAZY rest-frame V-band flux density uncertainty               | uJy
336 | ez_restJ            | EAZY rest-frame J-band flux density                           | uJy
337 | ez_restJ_err        | EAZY rest-frame J-band flux density uncertainty               | uJy
338 | ez_dL               | EAZY luminosity distance at ez_z_phot                         | Mpc
339 | ez_mass             | EAZY log stellar mass                                         | log(solMass)
340 | ez_sfr              | EAZY log SFR                                                  | log(solMass/yr)
341 | ez_ssfr             | EAZY log sSFR                                                 | log(yr**(-1))
342 | ez_Lv               | EAZY log V-band luminosity                                    | log(solLum)
343 | ez_LIR              | EAZY total 8-1000 um luminosity                               | solLum
344 | ez_energy_abs       | EAZY implied absorbed energy associated with Av               | solLum
345 | ez_Lu               | EAZY luminosity in rest-frame U band                          | solLum
346 | ez_Lj               | EAZY luminosity in rest-frame J band                          | solLum
347 | ez_L1400            | EAZY luminosity in tophat filter at 1400 A (200 A wide) rest-frame | solLum
348 | ez_L2800            | EAZY luminosity in tophat filter at 2800 A (200 A wide) rest-frame | solLum
349 | ez_LHa              | EAZY Halpha line luminosity (reddened)                        | solLum
350 | ez_LOIII            | EAZY [OIII] 4959+5007 line luminosity (reddened)              | solLum
351 | ez_LHb              | EAZY Hbeta line luminosity (reddened)                         | solLum
352 | ez_LOII             | EAZY [OII] 3726+3729 line luminosity (reddened)               | solLum
353 | ez_MLv              | EAZY mass-to-light ratio in V band                            | solMass/solLum
354 | ez_Av               | EAZY extinction in V band                                     | mag
355 | ez_lwAgeV           | EAZY light-weighted age in the V band                         | Gyr
356 | ez_mass_p025        | EAZY  2.5% percentile of log stellar mass                     | log(solMass)
357 | ez_mass_p160        | EAZY 16.0% percentile of log stellar mass                     | log(solMass)
358 | ez_mass_p500        | EAZY 50.0% percentile of log stellar mass                     | log(solMass)
359 | ez_mass_p840        | EAZY 84.0% percentile of log stellar mass                     | log(solMass)
360 | ez_mass_p975        | EAZY 97.5% percentile of log stellar mass                     | log(solMass)
361 | ez_sfr_p025         | EAZY  2.5% percentile of log SFR                              | log(solMass/yr)
362 | ez_sfr_p160         | EAZY 16.0% percentile of log SFR                              | log(solMass/yr)
363 | ez_sfr_p500         | EAZY 50.0% percentile of log SFR                              | log(solMass/yr)
364 | ez_sfr_p840         | EAZY 84.0% percentile of log SFR                              | log(solMass/yr)
365 | ez_sfr_p975         | EAZY 97.5% percentile of log SFR                              | log(solMass/yr)
366 | ez_Lv_p025          | EAZY  2.5% percentile of log V-band luminosity                | log(solLum)
367 | ez_Lv_p160          | EAZY 16.0% percentile of log V-band luminosity                | log(solLum)
368 | ez_Lv_p500          | EAZY 50.0% percentile of log V-band luminosity                | log(solLum)
369 | ez_Lv_p840          | EAZY 84.0% percentile of log V-band luminosity                | log(solLum)
370 | ez_Lv_p975          | EAZY 97.5% percentile of log V-band luminosity                | log(solLum)
371 | ez_LIR_p025         | EAZY  2.5% percentile of total 8-1000 um luminosity           | solLum
372 | ez_LIR_p160         | EAZY 16.0% percentile of total 8-1000 um luminosity           | solLum
373 | ez_LIR_p500         | EAZY 50.0% percentile of total 8-1000 um luminosity           | solLum
374 | ez_LIR_p840         | EAZY 84.0% percentile of total 8-1000 um luminosity           | solLum
375 | ez_LIR_p975         | EAZY 97.5% percentile of total 8-1000 um luminosity           | solLum
376 | ez_energy_abs_p025  | EAZY  2.5% percentile of implied absorbed energy associated with Av | solLum
377 | ez_energy_abs_p160  | EAZY 16.0% percentile of implied absorbed energy associated with Av | solLum
378 | ez_energy_abs_p500  | EAZY 50.0% percentile of implied absorbed energy associated with Av | solLum
379 | ez_energy_abs_p840  | EAZY 84.0% percentile of implied absorbed energy associated with Av | solLum
380 | ez_energy_abs_p975  | EAZY 97.5% percentile of implied absorbed energy associated with Av | solLum
381 | ez_Lu_p025          | EAZY  2.5% percentile of luminosity in rest-frame U band      | solLum
382 | ez_Lu_p160          | EAZY 16.0% percentile of luminosity in rest-frame U band      | solLum
383 | ez_Lu_p500          | EAZY 50.0% percentile of luminosity in rest-frame U band      | solLum
384 | ez_Lu_p840          | EAZY 84.0% percentile of luminosity in rest-frame U band      | solLum
385 | ez_Lu_p975          | EAZY 97.5% percentile of luminosity in rest-frame U band      | solLum
386 | ez_Lj_p025          | EAZY  2.5% percentile of luminosity in rest-frame J band      | solLum
387 | ez_Lj_p160          | EAZY 16.0% percentile of luminosity in rest-frame J band      | solLum
388 | ez_Lj_p500          | EAZY 50.0% percentile of luminosity in rest-frame J band      | solLum
389 | ez_Lj_p840          | EAZY 84.0% percentile of luminosity in rest-frame J band      | solLum
390 | ez_Lj_p975          | EAZY 97.5% percentile of luminosity in rest-frame J band      | solLum
391 | ez_L1400_p025       | EAZY  2.5% percentile of lum tophat filter at 1400 A (200 A wide) rf | solLum
392 | ez_L1400_p160       | EAZY 16.0% percentile of lum tophat filter at 1400 A (200 A wide) rf | solLum
393 | ez_L1400_p500       | EAZY 50.0% percentile of lum tophat filter at 1400 A (200 A wide) rf | solLum
394 | ez_L1400_p840       | EAZY 84.0% percentile of lum tophat filter at 1400 A (200 A wide) rf | solLum
```

```
395 | ez_L1400_p975     | EAZY 97.5% percentile of lum tophat filter at 1400 A (200 A wide) rf | solLum
396 | ez_L2800_p025     | EAZY  2.5% percentile of lum tophat filter at 2800 A (200 A wide) rf | solLum
397 | ez_L2800_p160     | EAZY 16.0% percentile of lum tophat filter at 2800 A (200 A wide) rf | solLum
398 | ez_L2800_p500     | EAZY 50.0% percentile of lum tophat filter at 2800 A (200 A wide) rf | solLum
399 | ez_L2800_p840     | EAZY 84.0% percentile of lum tophat filter at 2800 A (200 A wide) rf | solLum
400 | ez_L2800_p975     | EAZY 97.5% percentile of lum tophat filter at 2800 A (200 A wide) rf | solLum
401 | ez_LHa_p025       | EAZY  2.5% percentile of Halpha line luminosity (reddened)          | solLum
402 | ez_LHa_p160       | EAZY 16.0% percentile of Halpha line luminosity (reddened)          | solLum
403 | ez_LHa_p500       | EAZY 50.0% percentile of Halpha line luminosity (reddened)          | solLum
404 | ez_LHa_p840       | EAZY 84.0% percentile of Halpha line luminosity (reddened)          | solLum
405 | ez_LHa_p975       | EAZY 97.5% percentile of Halpha line luminosity (reddened)          | solLum
406 | ez_LOIII_p025     | EAZY  2.5% percentile of [OIII] 4959+5007 line luminosity (reddened) | solLum
407 | ez_LOIII_p160     | EAZY 16.0% percentile of [OIII] 4959+5007 line luminosity (reddened) | solLum
408 | ez_LOIII_p500     | EAZY 50.0% percentile of [OIII] 4959+5007 line luminosity (reddened) | solLum
409 | ez_LOIII_p840     | EAZY 84.0% percentile of [OIII] 4959+5007 line luminosity (reddened) | solLum
410 | ez_LOIII_p975     | EAZY 97.5% percentile of [OIII] 4959+5007 line luminosity (reddened) | solLum
411 | ez_LHb_p025       | EAZY  2.5% percentile of Hbeta line luminosity (reddened)           | solLum
412 | ez_LHb_p160       | EAZY 16.0% percentile of Hbeta line luminosity (reddened)           | solLum
413 | ez_LHb_p500       | EAZY 50.0% percentile of Hbeta line luminosity (reddened)           | solLum
414 | ez_LHb_p840       | EAZY 84.0% percentile of Hbeta line luminosity (reddened)           | solLum
415 | ez_LHb_p975       | EAZY 97.5% percentile of Hbeta line luminosity (reddened)           | solLum
416 | ez_LOII_p025      | EAZY  2.5% percentile of [OII] 3726+3729 line luminosity (reddened) | solLum
417 | ez_LOII_p160      | EAZY 16.0% percentile of [OII] 3726+3729 line luminosity (reddened) | solLum
418 | ez_LOII_p500      | EAZY 50.0% percentile of [OII] 3726+3729 line luminosity (reddened) | solLum
419 | ez_LOII_p840      | EAZY 84.0% percentile of [OII] 3726+3729 line luminosity (reddened) | solLum
420 | ez_LOII_p975      | EAZY 97.5% percentile of [OII] 3726+3729 line luminosity (reddened) | solLum
421 | ez_ssfr_p025      | EAZY  2.5% percentile of log sSFR                                   | log(yr**(-1))
422 | ez_ssfr_p160      | EAZY 16.0% percentile of log sSFR                                   | log(yr**(-1))
423 | ez_ssfr_p500      | EAZY 50.0% percentile of log sSFR                                   | log(yr**(-1))
424 | ez_ssfr_p840      | EAZY 84.0% percentile of log sSFR                                   | log(yr**(-1))
425 | ez_ssfr_p975      | EAZY 97.5% percentile of log sSFR                                   | log(yr**(-1))
426 | ez_Av_p025        | EAZY  2.5% percentile of extinction in V band                       | mag
427 | ez_Av_p160        | EAZY 16.0% percentile of extinction in V band                       | mag
428 | ez_Av_p500        | EAZY 50.0% percentile of extinction in V band                       | mag
429 | ez_Av_p840        | EAZY 84.0% percentile of extinction in V band                       | mag
430 | ez_Av_p975        | EAZY 97.5% percentile of extinction in V band                       | mag
```

References

Arnouts, S., Moscardini, L., Vanzella, E., et al. 2002, MNRAS, 329, 355

Astropy Collaboration, Price-Whelan, A. M., Sipőcz, B. M., et al. 2018, The Astronomical Journal, 156, 123, aDS Bibcode: 2018AJ....156..123A

Barbary, K. 2016, The Journal of Open Source Software, 1, 58

Bertin, E. & Arnouts, S. 1996, A&AS, 117, 393

Brammer, G. B., van Dokkum, P. G., & Coppi, P. 2008, ApJ, 686, 1503

Drlica-Wagner, A., Sevilla-Noarbe, I., Rykoff, E. S., et al. 2018, ApJS, 235, 33

Gaia Collaboration, Brown, A. G. A., Vallenari, A., et al. 2016, Astronomy & Astrophysics, 595, A2

Gaia Collaboration, Brown, A. G. A., Vallenari, A., et al. 2018, Astronomy & Astrophysics, 616, A1

Hsieh, B.-C., Wang, W.-H., Hsieh, C.-C., et al. 2012, The Astrophysical Journal Supplement Series, 203, 23

Ilbert, O., Arnouts, S., McCracken, H. J., et al. 2006, A&A, 457, 841

Laigle, C., McCracken, H. J., Ilbert, O., et al. 2016, ApJS, 224, 24

Lang, D., Hogg, D. W., & Mykytyn, D. 2016, Astrophysics Source Code Library, ascl:1604.008

McCracken, H. J., Milvang-Jensen, B., Dunlop, J., et al. 2012, Astronomy and Astrophysics, 544, A156

Robitaille, T. P., Tollerud, E. J., Greenfield, P., et al. 2013, Astronomy & Astrophysics, 558, A33, publisher: EDP Sciences

Taylor, M. B. 2006, in Astronomical Society of the Pacific Conference Series, Vol. 351, Astronomical Data Analysis Software and Systems XV, ed. C. Gabriel, C. Arviset, D. Ponz, & S. Enrique, 666

Weaver, J. R., Kauffmann, O. B., Ilbert, O., et al. 2022, ApJS, 258, 11